

Thermal and optical characterization of pigments attached to cellulose substrates by means of a self-normalized photoacoustic technique

J.A. Balderas-López, I.S. Martínez-López, M. León-Martínez, Y.M. Gómez y Gómez,
M.E. Bautista-Ramírez, A. Muñoz-Diosdado, and G. Gálvez-Coyt.
*Unidad Profesional Interdisciplinaria de Biotecnología del Instituto Politécnico Nacional,
Avenida Acueducto S/N, Col. Barrio la Laguna, Ticomán, México, D.F., 07340, México,
e-mail: abrahambalderas@hotmail.com*

J. Diaz-Reyes
*Centro de Investigación en Biotecnología Aplicada del Instituto Politécnico Nacional,
Ex-Hacienda de San Juan Molino Km. 1.5, Tepetitla, Tlaxcala, 90700, México.*

Recibido el 25 de febrero de 2009; aceptado el 18 de junio de 2009

A self-normalized photoacoustic (PA) methodology, involving the front and transmission configurations in the Beer-Lambert model for light absorption, is implemented for the measurement of optical and thermal properties of thin layers of substances in solid phase. To achieve this, the corresponding theoretical equations describing the PA effect in the Rosencwaig-Gersho model, were used. This new methodology was applied for the measurement of the optical absorption coefficient (at 658 nm) and thermal diffusivity of paper samples with different colors. This last physical property was also measured for all paper samples by using a self-normalized PA technique, already reported in the literature, involving the surface absorption model. In order to fulfill the theoretical assumptions in this last case, the paper samples were painted, on both sides, with a black marker. The thermal diffusivity values obtained in both cases were quite consistent among themselves and with the corresponding ones reported for similar materials.

Keywords: Photoacoustic; thermal; optical; pigments.

Se implementa una metodología fotoacústica (FA) auto-normalizada, la cual involucra las configuraciones frontal y por transmisión en el modelo de absorción luminosa de Beer-Lambert, para la medición de las propiedades ópticas y térmicas de láminas delgadas de sustancias en la fase sólida. Se utilizan para este fin las correspondientes ecuaciones teóricas que describen el efecto fotoacústico en el modelo de Rosencwaig-Gersho. Esta nueva metodología se empleó para la medición del coeficiente de absorción óptico (a 658 nm) y la difusividad térmica de muestras de papel de diferentes colores. Se midió también esta última propiedad térmica para todas las muestras de papel utilizando una técnica FA auto-normalizada, ya reportada en la literatura, en la cual se utiliza el modelo de absorción superficial. Para satisfacer los requerimientos teóricos en este último caso, las muestras de papel se pintaron con marcador negro en ambos lados. Los valores de difusividad térmica medidos en ambos casos estuvieron en excelente acuerdo entre ellos y con los correspondientes reportados en la literatura para materiales similares.

Descriptores: Fotoacústica; térmica; óptica; pigmentos.

PACS: 44.10.+i; 65.90.+i; 66.70-f.

1. Introduction

Two main photoacoustic (PA) configurations have been reported for thermal and optical characterization of substances in the condensed phase: the front configuration, which has been mainly used for optical characterization at fixed light modulation frequency, and the rear configuration (or transmission configuration) in which the PA signal, usually as a function of the modulation frequency, has been mainly employed for thermal diffusivity measurements. [1 - 4] However, the use of the PA signal in the modulation frequency domain faces the problem of the transfer function, which is the system's electronics response to this variable; thus in this domain it is necessary to use an adequate normalization procedure in order to obtain confident results. Balderas-López and Mandelis [5,7] introduced for this goal the so-called self-normalization procedure, which consists in taking the signal's ratio in the transmission and front configurations, eliminating the transfer function. This self-normalization procedure

has an additional advantage if the sample's light surface absorption model is fulfilled, since it provides a simple expression from which only the sample's thermal diffusivity can be obtained; it has been applied in this way for the measurement of thermal diffusivity of very strong light absorbers as metals and black paints. [5,7,8] In order to apply this self-normalization procedure to other kinds of single-layered materials, a more general sample's light absorption model is needed, and the Beer-Lambert's law for light absorption is adequate for this purpose. Thus the analytical expressions for the front and rear PA configurations in the Beer-Lambert model for light absorption are described in order to obtain the corresponding self-normalized expression, which is useful for optical characterization of materials in the condensed phase. The thermal diffusivity and the optical absorption coefficient (at 658 nm) of papers of different colors (blue, green and black) were measured to show the capabilities of this more general self-normalized methodology; in addition, the present work describes some experimental cri-

teria, to distinguish samples in the surface absorption limit (very large optical absorption coefficient) and to select the appropriate modulation frequency range for reliable analysis.

2. Theory

The geometry of the one-dimensional model, depicted in Fig. 1, consists of a single-layered material, *m*, embedded in an optically non-absorbing media *g*. If monochromatic radiation, with intensity I_0 and modulation frequency f (angular modulation frequency $\omega = 2\pi f$), strikes medium *m* and it is absorbed through it according to the Beer-Lambert model, the set of differential equations for the corresponding one-dimensional heat diffusion problem is

$$\begin{aligned} \frac{\partial^2 T_g}{\partial x^2} - \frac{1}{\alpha_g} \frac{\partial T_g}{\partial t} &= 0 & 0 \leq x \\ \frac{\partial^2 T_m}{\partial x^2} - \frac{1}{\alpha_m} \frac{\partial T_m}{\partial t} &= -\frac{\beta I_0}{k_m} e^{\beta x} e^{i\omega t} & -l \leq x \leq 0 \quad (1) \\ \frac{\partial^2 T_g}{\partial x^2} - \frac{1}{\alpha_g} \frac{\partial T_g}{\partial t} &= 0 & -\infty < x \leq -l \end{aligned}$$

subject to the boundary conditions of heat flux and temperature continuity at the interfaces *g-m*, and *m-g*:

$$\begin{aligned} T_g(0, t) &= T_m(0, t) \\ T_m(-l, t) &= T_g(-l, t) \\ -k_g \frac{\partial T_g}{\partial x}(0, t) &= -k_m \frac{\partial T_m}{\partial x}(0, t) \\ -k_m \frac{\partial T_m}{\partial x}(-l, t) &= -k_g \frac{\partial T_g}{\partial x}(-l, t) \end{aligned}$$

and the physical requirement of finite solutions as $x \rightarrow \pm\infty$.

In these equations T_j , α_j , and k_j , $j = m, g$, correspond, respectively, to the temperature, thermal diffusivity and thermal conductivity of medium *j*; β is the optical absorption coefficient of the absorbing medium *m*, which has a thickness l .

According to the Rosencwaig-Gersho model [1] for a gas-cell PA setup, the PA signal is proportional to the temperature fluctuations at the interface between the medium which seals the PA chamber and the gas inside it. Assuming medium *g* in Fig. 1 as this gas, the PA signal in the transmission configuration is then proportional to $T_m(-l, t)$ and the corresponding one for the front configuration is proportional to $T_m(0, t)$. These PA signals are given, respectively, by [6,7]

$$\delta P_T(f) = KG(f) \frac{I_0}{k_m \sigma_m} \frac{r}{(1-r^2)} \left[\frac{(1+b_{gm})(1+r)e^{-\beta l} e^{\sigma_m l} - 2(r+b_{gm}) - (1-b_{gm})(1-r)e^{-\beta l} e^{-\sigma_m l}}{(1+b_{gm})^2 e^{\sigma_m l} - (1-b_{gm})^2 e^{-\sigma_m l}} \right] \quad (2)$$

$$\delta P_F(f) = KG(f) \frac{I_0}{k_m \sigma_m} \frac{r}{(1-r^2)} \left[\frac{(1+b_{gm})(1-r)e^{\sigma_m l} + 2(r-b_{gm})e^{-\beta l} - (1-b_{gm})(1+r)e^{-\sigma_m l}}{(1+b_{gm})^2 e^{\sigma_m l} - (1-b_{gm})^2 e^{-\sigma_m l}} \right] \quad (3)$$

In these two equations, σ_m , b_{gm} and r are given, respectively, by $\sigma_m = (1+i)(\pi f/\alpha_m)^{1/2}$, $b_{gm} = e_g/e_m$ and $r = \beta/\sigma_m$, where e_j , $j = g, m$ is the thermal effusivity of media *j*. K is a geometrical factor that depends on both the PA chamber's size and the thermal properties of the gas inside it; finally, $G(f)$ represents the transfer function.

Self-Normalization Procedure

The self-normalized PA signal, denoted here as $\delta P_N(f)$, is obtained as the ratio of the PA signal for the transmission configuration and the corresponding one for the front configuration as $\delta P_N(f) = \delta P_T(f)/\delta P_F(f)$. This procedure clearly eliminates the common global factor in Eqs. (2) and (3), in particular the geometrical factor K and the transfer function $G(f)$, resulting in the normalized expression

$$\delta P_N(f) = \frac{(1+b_{gm})(1+r)e^{-\beta l} e^{\sigma_m l} - 2(r+b_{gm}) - (1-b_{gm})(1-r)e^{-\beta l} e^{-\sigma_m l}}{(1+b_{gm})(1-r)e^{\sigma_m l} + 2(r-b_{gm})e^{-\beta l} - (1-b_{gm})(1+r)e^{-\sigma_m l}} \quad (4)$$

It is then possible, at least in principle, to get information on the sample's thermal and optical properties by an adequate analysis of Eq. (4). This is, in general, a very difficult task, unless the appropriate limiting conditions on the optical and thermal properties of the sample *m* are taken. There are two especially useful limiting conditions:

A. Sample *m* in the thermally thick regime (Thermo-Optical limit)

In the thermally thick regime for the sample *m*, $|\sigma_m l| \gg 1$ ($|\exp(-\sigma_m l)| \approx 0$). If, in addition, not too large value for the

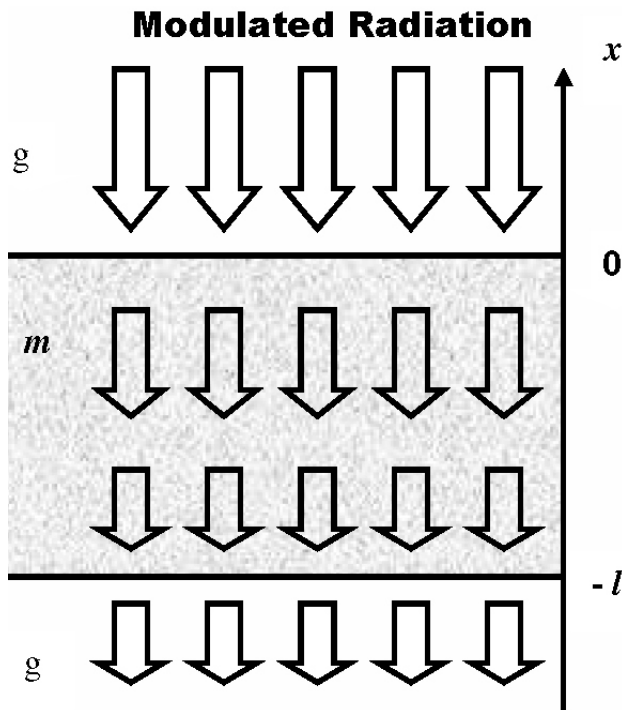


FIGURE 1. Schematic representation of the one-dimensional mathematical heat diffusion model. Medium *m* is assumed to absorb light by following the Beer-Lambert model, with optical absorption coefficient β .

optical absorption coefficient β is assumed, Eq. (4) takes on the simpler expression

$$\delta P_N(f) = \frac{(1+r)}{(1-r)} e^{-\beta l}. \tag{5}$$

The amplitude, $R(f)$, and tangent of the phase, $\Phi(f)$, of this last equation can be written, respectively, as:

$$R(f) = e^{-\beta l} \frac{\sqrt{1 + \frac{1}{4} \left(\frac{P}{\sqrt{f}}\right)^4}}{\sqrt{1 - \frac{P}{\sqrt{f}} + \frac{1}{2} \left(\frac{P}{\sqrt{f}}\right)^2}} \tag{6a}$$

$$\tan(\Phi(f)) = -\frac{\frac{P}{\sqrt{f}}}{1 - \frac{1}{2} \left(\frac{P}{\sqrt{f}}\right)^2} \tag{6b}$$

where $P = \beta(\alpha_m/\pi)^{1/2}$, Eq. (6a) behaves asymptotically as $\exp(-\beta l)$ and, at least in principle, it is possible to obtain the optical absorption coefficient β by means of the experimental measurement of this asymptotic value; this is, however, a difficult task since the photoacoustic signal is strongly affected by thermoelastic mechanisms in the high modulation frequency range. Moreover, the PA amplitude is also influenced by light intensity fluctuations. The phase is more convenient for analytical purposes since it is not affected by light source fluctuations; $\tan(\Phi)$ has, in addition, a very simple structure in this case and it is possible to obtain qualitative information regarding its expected analytical behavior which depends on the value of the parameter P . For P -values in the thermally thick regime such that $(2f)^{1/2} > P$, $\tan(\Phi)$ has no critical values or inflection points in this range. This means, in particular, that it is a continuous, monotonically increasing function with concavity downwards. A P -value is also possible, especially for a large optical absorption coefficient in the thermally thick regime, for which $(2f)^{1/2} < P$; as the modulation frequency increases in this last case, $\tan(\Phi)$ goes through some discontinuities (when the phase Φ takes on the $\pi/2$ -value), the first one occurring at a modulation frequency given by

$$f_d = \frac{\beta^2 \alpha_m}{2\pi}. \tag{7}$$

TABLE I. Thermal diffusivities and optical absorption coefficient as measured for each of the paper samples used in this work. $\alpha_{ph,op}$ and $\alpha_{tan,op}$ refer, respectively, to the thermal diffusivity from the phase, Φ , and $\tan(\Phi)$, for those samples which were in the thermal limit and $\alpha_{ph,te}$ and $\alpha_{tan,te}$ refer to the corresponding ones for all samples as they were black-painted; β refers to the sample's optical absorption coefficient.

Paper Sample	Thickness (cm)	$\alpha_{tan,op}$ (cm ² /s)	$\alpha_{ph,op}$ (cm ² /s)	$\alpha_{tan,te}$ (cm ² /s)	$\alpha_{ph,te}$ (cm ² /s)	β (cm ⁻¹)
B1	0.0110, 0.0118	—	—	0.0028	0.0028	107
B2	0.0116, 0.0128	—	—	0.0017	0.0019	144
B3	0.0095, 0.0096	0.0016	0.0016	0.0019	0.0019	—
B4	0.0095, 0.0100	0.0014	0.0014	0.0015	0.0015	—
G1	0.0105, 0.0108	—	—	0.0012	0.0012	168
G2	0.0102, 0.0101	—	—	0.0018	0.0016	95
G3	0.0133, 0.0132	—	—	0.0022	0.0023	151
G4	0.0117, 0.0112	—	—	0.0016	0.0017	126
Black	0.0117, 0.0117	0.0024	0.0023	0.0024	0.0023	—

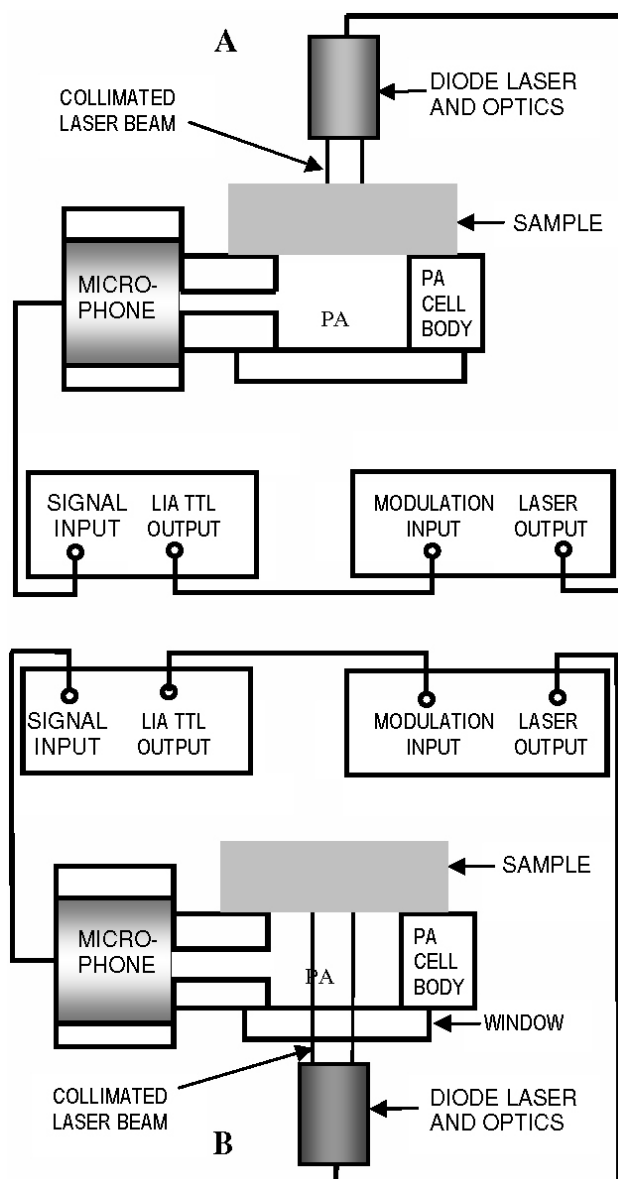


FIGURE 2. Schematic cross-section of the photoacoustic (PA) experimental setup. A. PA transmission configuration. B. PA front configuration.

If experimentally this last case occurs, it has to be analyzed with care since Eq. (5), which was obtained by assuming not too large β -values, might not be valid anymore. From the parameter P in Eq. (6b) and from f_d in Eq. (7), the optical absorption coefficient can be obtained as soon as the sample's thermal diffusivity is determined. Two main characteristics of Eq. (6b) are the absence of zeros, and its asymptotic behavior, $\tan(\Phi) \rightarrow 0$, as $f \rightarrow \infty$, since these facts provide important criteria for distinguishing a given sample in this first limit. The asymptotic behavior, in particular, can also be used as a tool for selection of the modulation frequency range for analysis, since thermoelastic contributions significantly affect the PA signal in the thermally thick regime. This first case is named in this work the Thermo-Optical limit since both the optical absorption coefficient and the thermal

diffusivity are involved in the PA signal, in contrast to the next limiting case which, as will be shown later, only involves thermal properties.

B. Very high optically opaque sample m (Thermal Limit)

If an infinite sample's optical absorption coefficient is assumed: $\beta \rightarrow \infty$ and $r \rightarrow \infty$, taking the appropriate mathematical limits, [2,8] Eq. (4) can be written as

$$\delta P_N(f) = (1 + \gamma_{gm}) \frac{e^{-\sigma_m l}}{[1 + \gamma_{gm} e^{-2\sigma_m l}]} \quad (8)$$

where $\gamma_{gm} = (1 - b_{gm}) / (1 + b_{gm})$. This last equation holds for the self-normalized PA signal in the surface absorption model and it has been already reported by Balderas-López [8]. Equation (8) has been successfully used to provide various PA self-normalized methodologies to measure the thermal diffusivity of thin metallic foils [8] and other highly opaque samples [9] from $\tan(\Phi)$, which can be written in this case as

$$\tan(\Phi) = -\tanh(x) \tan(x) \quad (9)$$

where $x = (\pi f / \alpha_m)^{1/2} l$, and from the phase, which, in the sample's thermally thick regime, can be written as

$$\Phi = - \left(\sqrt{\frac{\pi}{\alpha_m}} \right) \sqrt{f}. \quad (10)$$

Equation (9) shows discontinuities and zeros; the first discontinuity takes place at a modulation frequency given by

$$f_d = \frac{\pi \alpha_m}{4l^2}. \quad (11)$$

The sample's thermal diffusivity can be measured from these two last equations, for Eq. (10) by means of the parameter $m = (\pi / \alpha_m)^{1/2} l$, which is the slope of the straight line obtained from a linear fitting procedure on Eq. (10), and for Eq. (11) by means of the modulation frequency value where the first discontinuity takes place.

Since Eq. (8) depends only on thermal parameters and it permits the measurement of the sample's thermal diffusivity, this limit is named here as the thermal limit.

3. Experimental

The experimental PA set-up, shown in Fig. 2, consisted of a red (658 nm) diode laser (Hitachi HL6535MG) intensity-modulated by means of a laser diode controller (Thorlabs model LCD-202B) which was driven by means of the TTL (Transistor-Transistor-Logic) internal lockin output (Stanford Research Systems, model SR 830). Both PA configurations were obtained, once the sample was in place, by just shifting the diode laser head to the corresponding side of the PA chamber; Fig. 2a shows a schematic cross-section of the PA transmission configuration, and the corresponding front configuration is shown in Fig. 2b. The samples consisted

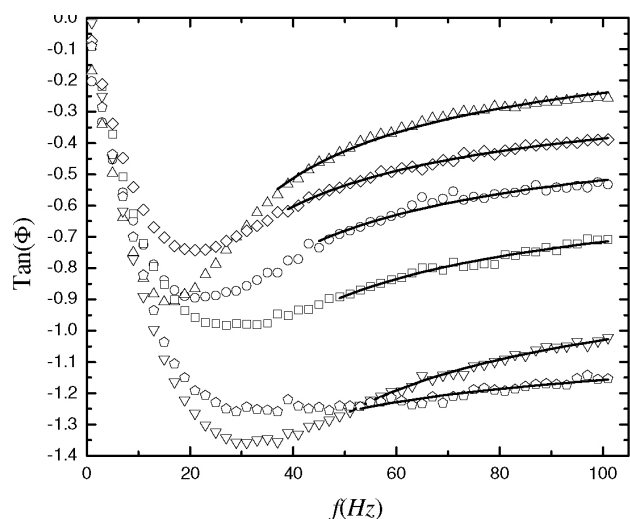


FIGURE 3. Experimental behavior of Tangent of the normalized phase, as a function of the modulation frequency, for six of the paper samples listed in Table I. Circles (O) correspond to sample B1, thickness 0.0110 cm; squares (◻) correspond to sample G1, thickness 0.0105 cm; triangles up (Δ) correspond to sample B2, thickness 0.0116 cm; triangles down (∇) correspond to sample G3, thickness 0.0133 cm; diamonds (◊) correspond to sample G4, thickness 0.0117 cm and pentagons (◑) correspond to sample G2, thickness 0.0102 cm.

of paper sheets, black and with different intensities of green and blue colors, cut in 2 cm, squares. The blue samples were labeled B1 to B4 and the green ones G1 to G4 (Table I, column 1). The PA signal for each specimen in both PA configurations was recorded as a function of the modulation frequency (modulation frequency scan), in a range of 1 Hz to 101 Hz, in steps of 2 Hz. Regarding the analytical procedure, the difference of PA phases (the phase for the transmission configuration minus the corresponding one for the front configuration) were calculated for each of the different modulation frequencies and then the tangent for each normalized data was obtained.

4. Results and Discussion

Figure 3 shows $\tan(\Phi)$ as a function of the modulation frequency, for six of the paper samples, labeled in Table I B1, B2, G1, G2, G3 and G4, which resulted in the thermo-optical limit (IIA). The fitting procedure of $\tan(\Phi)$ to Eq. (6b) (continuous lines on the same figure) in the sample's thermally thick regime yielded the parameter $P = \beta(\alpha_m/\pi)^{1/2}$, as discussed above. Figs. 4a and 4b show the corresponding plots for $\tan(\Phi)$ and $\Phi(f)$, respectively, for the other paper samples, labeled in Table I B3, B4 and Black, which resulted in the thermal limit (IIB). This time the sample's thermal diffusivity was obtained by means of the analytical procedures described in Sec. IIB. Figure 4a shows the modulation frequency values where the first discontinuity took place; these values were used for thermal diffusivity evaluation through

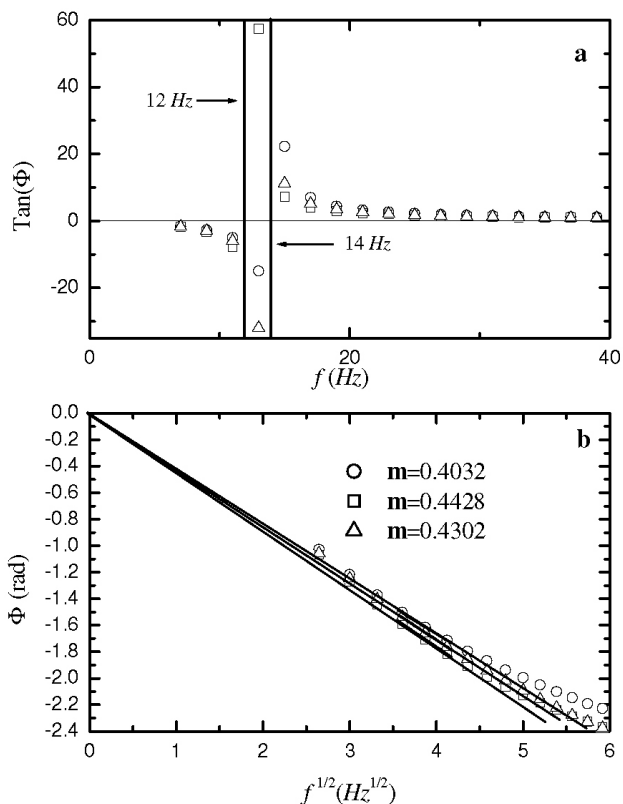


FIGURE 4. **a.** Experimental behavior of Tangent of the Photoacoustic phase, $\Phi(f)$, as a function of the modulation frequency, for three of the paper samples listed in Table I Circles (O) correspond to sample B3, thickness 0.0095 cm, squares (◻) correspond to sample B4, thickness 0.0095 cm, and triangles (Δ) correspond to the black sample, thickness 0.0117 cm. The modulation frequency values where the corresponding discontinuities took place are shown on the sample plot. **b.** Normalized Photoacoustic phase, $\Phi(f)$, as a function of the root square of the modulation frequency, for the same samples as shown in **a**. Continuous lines are the best fits to linear models; the corresponding slopes are shown on the same plot.

Eq. (11), and the results are summarized in Table I, column 3. Figure 4b shows, as continuous lines, the linear fits of $\Phi(f)$ from Eq. (10) in the thermally thick regime (dot lines were used as guidelines, as described in Ref. 8), and the corresponding thermal diffusivities were evaluated from the slopes, shown on the same plot, as described in Sec. IIB; the corresponding values are summarized in Table I, column 4. The first sample's thicknesses, summarized in Table I, column 2, were used in both cases. In order to obtain thermal diffusivities for all the samples (especially for those in the optical limit) and, at the same time, to have another independent evaluation of thermal diffusivities for the samples in the thermal limit, the same experiment was done for the samples, this time black-painted on both sides with a black marker, to eliminate any optical influence on the PA signal. Figures 5a and 5b show the corresponding plots for the samples B1, B2 and G3, for $\tan(\Phi)$ and Φ , respectively. The analysis was done by following the analytical procedure described in Sec. IIB, for high light absorbers. Table I, columns 5 and 6,

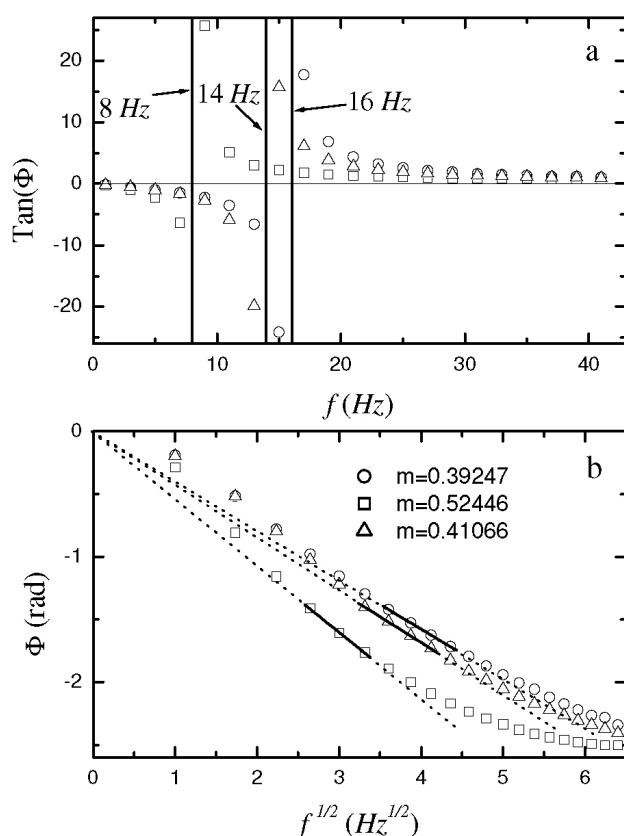


FIGURE 5. **a.** Experimental behavior of Tangent of the Photoacoustic phase, $\Phi(f)$, as a function of the modulation frequency, for three of the paper samples listed in Table I. Samples were black-painted on both sides to eliminate any optical influence on the photoacoustic signal. Circles (○) correspond to sample B1, thickness 0.0118 cm, squares (□) correspond to sample B2, thickness 0.0128 cm, and triangles (△) correspond to sample G4, thickness 0.0112 cm. The modulation frequency values where the corresponding discontinuities took place are shown on the sample plot. **b.** Normalized Photoacoustic phase, $\Phi(f)$, as a function of the root square of the modulation frequency, for the same samples as shown in **a.** The continuous lines are the best fits to linear models; the corresponding slopes are shown on the same plot.

summarize all the corresponding results for all paper samples studied in this work; this time the second sample's thicknesses, summarized in Table I, column 2, were used in both cases. The thermal diffusivities obtained with this procedure were used for optical absorption coefficient evaluation for those samples which were in the optical limit by means of the parameter P and Eq. (11). The corresponding optical absorption coefficients are summarized in Table I, column 7. It is interesting to note that the thermal diffusivities obtained for the samples in the thermal limit, and the corresponding ones painted with black, turned out to be very similar to each other, showing that the presence of the ink does not produce significant alteration of this thermal property.

5. Conclusions

A self-normalized PA methodology for measuring thermal and optical properties of pigments attached to cellulose substrates has been introduced. It can be used for color quantification for this kind of material through the direct measurement of the optical absorption coefficient. Although it has been applied here to paper, this new PA methodology has general application since it can be used for the measurement of thermal and optical properties of any kind of material. Since the sample's optical absorption coefficient can be measured, the pigment's concentration can be obtained once an appropriate calibration curve is constructed, in a very similar way to that used for quantification of pigments in liquids by means of commercial spectrophotometers.

Acknowledgments

The authors thank SIP-IPN, COFAA-IPN and CONACyT for their support.

1. A. Rosencwaig and A. Gersho, *J. Appl. Phys.* **47** (1976) 64.
2. J.A. Balderas-López, *Rev. Sci. Instrum.* **79** (2008) 024901.
3. C.A.S. Lima *et al.*, *Meas. Sci. Technol.* **11** (2000) 504.
4. L. Olenka, A.N. Medina, M.L. Baesso, A.C. Bento, and A.F. Rubira, *Brazilian Journal of Physics* **32** (2002) 516.
5. J.A. Balderas-López and A. Mandelis, *Rev. Sci. Instrum.* **74** (2003) 5219.
6. B. Bonno, J.L. Laporte, and Y. Rousset, *J. Appl. Phys.* **67**(1990) 2253.
7. A.C. Bento, D.T. Dias, L. Olenka, A.N. Medina, and M.L. Baesso, *Brazilian Journal of Physics* **32** (2002) 483.
8. J.A. Balderas-López, *Rev. Mex. Fís.* **74** (2004) 120.
9. J.A. Balderas-López, *Eur. Phys. J.* **153** (2008) 167.